

**Coherent propagation of laser beams in a small-sized system of weakly coupled optical light guides**A. A. Balakin,<sup>\*</sup> S. A. Skobelev, E. A. Anashkina, A. V. Andrianov, and A. G. Litvak*Institute of Applied Physics RAS, 603950 Nizhny Novgorod, Russia*

(Received 24 July 2018; published 31 October 2018)

The features of the self-action of a wave field in a small-sized optical system consisting of  $2N$  identical light guides, which are disposed equidistantly along a ring, and an isolated fiber in the center are studied analytically and numerically. Stable exact solutions are found for intense wave beams in such a system, allowing long-distance coherent transport of radiation in a set of optical fibers. The total beam power in this case can exceed several times the critical power of self-focusing in the continuous medium. This is clearly manifested for the out-of-phase spatial distribution of  $u_n = (-1)^n f$ , which is stable at arbitrary powers. Direct numerical simulation of the nonlinear unidirectional wave propagation equation confirms the stability of found wave field distributions.

DOI: [10.1103/PhysRevA.98.043857](https://doi.org/10.1103/PhysRevA.98.043857)**I. INTRODUCTION**

The successful development of fiber-optic technologies in recent decades has stimulated research on replacement of the components of solid-state laser systems by fiber components, which can radically change attractiveness of relevant applications. Although inferior to the solid-state systems from the viewpoint of their power characteristics, fiber lasers and nonlinear optical devices have such advantages as high efficiency of conversion of the pump energy into the radiation energy associated with the light-guide geometry and high quality of the spatial profile of the laser beam, as well as the low cost, small size, and lack of necessity to perform alignment in the process of operation. Note that the maximum achievable radiation power in a single fiber is limited primarily by the self-focusing process and nonlinear absorption in the medium, which leads to fiber damage.

Recently, the idea of amplifying wave packets in an array of independent light guides [1,2] is being discussed as a way to obtain laser pulses with an extremely high power level. Recent works [3,4] experimentally demonstrate the possibility of synchronizing laser radiation at the output of an array of independent optical fibers. One of the difficulties of the proposed approach is the high sensitivity of the method of coherent combining of fields with respect to various nonlinear perturbing factors.

The use of a multicore fiber (MCF) consisting of identical equidistantly disposed weakly coupled cores allows for initially coherent propagation of laser radiation with a total power being significantly higher than that capable of being transmitted in the single core. This stimulates the study of nonlinear wave processes in spatially periodic media, i.e., a set of weakly coupled light guides [5–7]. A number of interesting results were obtained in this field, in particular, the possibility of generating a supercontinuum [8,9] and shortening the laser pulse duration [10–12], controlling the structure of the wave field, and forming of light bullets [12–15]. However, as shown

by theoretical and experimental studies, in the system under consideration there exists its own critical power [16–18], at which self-focusing of the quasihomogeneous wave-field distribution and its fibrillation into a set of incoherent structures occurs [11].

In this paper, the theory of self-action of the wave field in the little studied case of small-sized discrete systems is developed for the purposes of transporting coherent laser radiation with a total power much higher than the critical self-focusing power in the medium. As a specific example, we consider propagation of laser beams in a multicore fiber, which is an array of  $2N$  identical cores surrounding the central core (see the example in Fig. 1). The value of  $N$  is rarely very large due to technological limitations in the production of an array of coupled light guides. It is known [19,20] that homogeneous wave-field distributions in such MCFs are unstable with respect to azimuth disturbances at a high beam power. In our work, inhomogeneous stationary nonlinear distributions of the wave field are found and their stability is demonstrated even at the total power being much higher than the critical self-focusing power. Direct numerical simulation of the nonlinear unidirectional wave propagation equation confirm the stability of found nonlinear distributions.

The paper is organized as follows. The basic equations are formulated in Sec. II. Their solutions in the linear limit are given in Sec. III. Nonlinear isotropic distributions of the wave field are considered in Sec. IV. Section V is devoted to mirror-symmetric nonlinear solutions. Amplitude-rugged nonlinear solutions (the “crown”) are considered in Sec. VI. The phase-modulated nonlinear mode and analysis of its stability are presented in Sec. VII. Section VIII contains the comparison of found analytical solutions with results of direct numerical simulation of the nonlinear unidirectional wave propagation equation.

**II. BASIC EQUATIONS**

Let us consider self-action of wave beams in a multicore fiber, which is an array of  $2N$  identical cores surrounding the central core. Figure 1 shows schematically this MCF fiber

<sup>\*</sup>balakin@appl.sci-nnov.ru

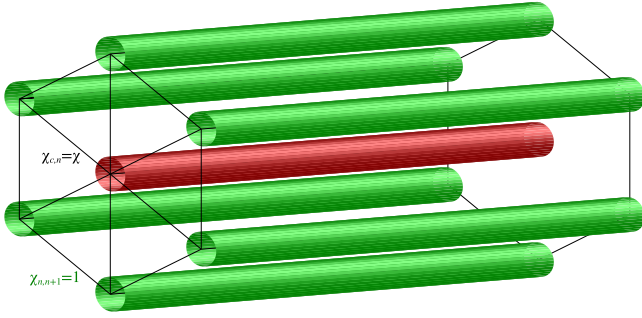


FIG. 1. Schematic representation of MCF with cores located equidistantly around the central one.

with  $N = 3$ . The analysis of this problem will be carried out on the basis of the standard theoretical model [6,11,17,18,21], where it is assumed that the fundamental directional modes of the optical cores oriented parallel to the  $z$  axis are weakly coupled. In this case, propagation of laser radiation in a multicore fiber can be described approximately as a superposition of the modes localized in each core:

$$\mathcal{E}(z, x, y) \simeq \sum_n \mathcal{A}_n(z) \mathcal{F}(x - x_n, y - y_n) e^{ik_n z} + \text{c.c.}, \quad (1)$$

where  $\mathcal{F}$  is the structure of the fundamental spatial mode in the core and  $\mathcal{A}_n$  is the envelope of the electric field in the  $n$ th core, which varies slowly along the  $z$  axis. The evolution of the envelope in the  $n$ th core during the propagation of a wave field along the  $z$  axis can be influenced by the Kerr nonlinearity of a single core and its interaction with the nearest-neighboring cores, which arises from the weak overlap of the modes directed by them. Assuming that the connections between the cores are weak and do not perturb the structure of the fundamental mode, we obtain the following system of equations for the envelope of the electric field  $\mathcal{A}_n$  in the  $n$ th core:

$$i \frac{\partial \mathcal{A}_n}{\partial z} = \beta_n |\mathcal{A}_n|^2 \mathcal{A}_n + \sum_{m=0}^{2N} \chi_{mn} \mathcal{A}_m. \quad (2)$$

Here, the index  $n$  changes from zero to  $2N$ , the parameter  $\beta_n$  is the coefficient of nonlinearity in the  $n$ th core, the coefficient  $\chi_{mn} = \chi_{nm}$  determines the connection strength between the  $m$ th and  $n$ th cores, and  $\chi_{nn} = k_n$  is the wave number in the  $n$ th core.

We assume that all the cores are identical, i.e., the wave number  $k_n = \chi_{nn}$ , the nonlinearity coefficients  $\beta_n$ , and the coupling coefficients ( $\chi_{n,n+1}$ ,  $\chi_{n,0}$  for  $n > 0$ ) are the same for all the cores. Then, the change in the variables  $u_n = \mathcal{A}_n e^{ik_n z} \sqrt{\beta_n / \chi_{n,n+1}}$  and the evolutionary coordinate  $z \rightarrow z \chi_{n,n+1}$  leads to the following system of equations for the complex field amplitudes:

$$i \frac{\partial a}{\partial z} = \chi \sum_{n=1}^{2N} u_n + |a|^2 a, \quad (3a)$$

$$i \frac{\partial u_n}{\partial z} = \chi a + u_{n+1} + u_{n-1} + |u_n|^2 u_n. \quad (3b)$$

Here,  $a = u_0$  and  $u_n$  are the amplitudes in the central and  $n$ th cores, respectively, and  $\chi = \chi_{n,0} / \chi_{n,n+1}$  is the normalized coefficient of connection to the central core. Equations (3) preserve the total power of the wave beam

$$\mathcal{P} = |a|^2 + \sum_{n=1}^{2N} |u_n|^2 = \text{const.} \quad (4)$$

The applicability of Eqs. (3) is limited by the applicability of the approximation of the single-mode propagation of the wave field in each core. It will be violated when the nonlinear wave-number shift  $\beta_n |\mathcal{A}_n|^2$  will be of the order of the gap between the fundamental and the second modes. It will occur [22] (see also Fig. 7) when the radiation power  $P_n = |\mathcal{A}_n|^2 \iint |\mathcal{F}|^2 dx dy$  in any core approaches the critical self-focusing power in the medium, i.e., at

$$|u_n|^2 = \frac{\beta_n}{\chi_{n,n+1}} \frac{P_n}{\iint |\mathcal{F}|^2 dx dy} \gtrsim \frac{4\pi}{\chi_{n,n+1} \iint |\mathcal{F}|^2 dx dy} \ggg 1. \quad (5)$$

Here, the small factor  $\chi_{n,n+1} \iint |\mathcal{F}|^2 dx dy \ll 1$  determines the degree of localization of the fundamental mode on the scale of the distance between the cores.

### III. LINEAR CASE

We turn first to analysis of Eqs. (3) in the linear case ( $|u_n|^2, |a|^2 \ll 1$ ). Due to the homogeneity of the equations, the solution in this limit is sought conveniently in the form of an expansion in the Bloch functions

$$u_n(z) = \sum_m f_m(z) e^{i\chi_m n}, \quad \chi_m = \frac{\pi m}{N}. \quad (6)$$

Substituting expression (6) into the system of equations (3), we obtain equations for the amplitude  $f_m(z)$  of the modes:<sup>1</sup>

$$i \frac{\partial f_m}{\partial z} = -2 \cos(\chi_m) f_m, \quad m \neq 0, \quad (7a)$$

$$i \frac{\partial a}{\partial z} = 2N \chi f_0, \quad (7b)$$

$$i \frac{\partial f_0}{\partial z} = \chi a + 2f_0. \quad (7c)$$

It is clear from Eqs. (7) that, in the linear case, the evolution of the amplitudes of the modes with  $m \neq 0$ ,

$$f_m(z) = e^{-ih_m z} f_m^{(0)}, \quad f_m^{(0)} \equiv f_m(z=0), \quad (8)$$

splits off from the dynamics of the wave field in the central core  $a$  and the averaged field  $f_0$  on the ring. Here, the value  $h_m = 2 \cos(\chi_m)$  plays the role of the inherent “wave number” of the  $m$ th mode.

Equations (7b) and (7c) have the form of an oscillator equation for the complex amplitudes  $a$  and  $f_0$ , and describe the periodic transfer of energy (“beats”) between the central core  $a$  and the averaged field on the ring  $f_0$  of the multicore fiber. The general solution of Eqs. (7b) and (7c) can be

<sup>1</sup>Here and in what follows, by “modes” we mean the distributions (eigenmodes) in the discrete linear problem.

represented as a superposition of normal oscillations with eigenfrequencies  $\lambda_{1,2} = 1 \pm \sqrt{1 + 2N\chi^2}$ :

$$a(z) = J_+ e^{-i\lambda_1 z} + J_- e^{-i\lambda_2 z}, \quad (9a)$$

$$f_0(z) = -\frac{\chi J_+}{\lambda_2} e^{-i\lambda_1 z} - \frac{\chi J_-}{\lambda_1} e^{-i\lambda_2 z}. \quad (9b)$$

Here,  $J_+$  and  $J_-$  are found based on the initial values of the wave field in the central core  $a^{(0)}$  and the averaged field on the ring  $f_0^{(0)}$  of the multicore optical fiber

$$J_{\pm} = \frac{\pm \chi N}{\pi(\lambda_1 - \lambda_2)} \left[ \frac{\chi a^{(0)}}{\lambda_{1,2}} \pm f_0^{(0)} \right]. \quad (10)$$

Analogous solutions (8) and (9) of a linear problem with  $N = 3$  were found in [23].

It follows from the analysis of formulas (9) and (10) that injection into the MCF of a specially prepared initial distribution of the wave field

$$a^{(0)} = -\frac{\lambda_1}{\chi} f_0^{(0)}, \quad (11a)$$

$$a^{(0)} = -\frac{\lambda_2}{\chi} f_0^{(0)} \quad (11b)$$

will result in zero coefficients  $J_+$  [for the case of Eq. (11a)] or  $J_-$  [for the case of Eq. (11b)]. Consequently, there will be no ‘‘beats,’’ and the distribution of the wave field will remain unchanged for wave field distributions (11).

The cubic nonlinearity of the medium will disrupt coherent propagation of high-power laser beams in the MCF. However, as will be shown below, the wave structures containing a small number of linear modes will be exact stable solutions in the nonlinear case as well. Therefore, we investigate various configurations of the spatial distribution of the wave field to ensure coherent radiation propagation in the MCF under consideration.

#### IV. ISOTROPIC DISTRIBUTIONS

Let us consider the case of uniform distribution of the wave field over the ring ( $f_{m \neq 0} = 0$ ). In this case, the system of equations (3) will take the form

$$i \frac{\partial a}{\partial z} = 2N\chi f_0 + |a|^2 a, \quad (12a)$$

$$i \frac{\partial f_0}{\partial z} = \chi a + 2f_0 + |f_0|^2 f_0. \quad (12b)$$

Resulting Eqs. (12) are the equations for two nonlinear oscillators with a linear connection between them. The system of equations (12) obviously preserves the total power of the wave beam

$$\mathcal{P} = |a|^2 + 2N|f_0|^2 = \text{const}. \quad (13)$$

##### A. MCF with no central core ( $\chi = 0$ )

First, we consider the simplest case. Suppose there is no central core ( $\chi = 0$ ). Then, the solution of the system of equations (12) has the form

$$a = 0, \quad u_n = f_0 e^{-i(2+|f_0|^2)z}. \quad (14)$$

Unfortunately, this solution will be stable only at a low power level. Indeed, for a field with perturbations of the form

$$u_n = [f_0 + \delta_m e^{i\lambda_m z + i\chi_m n}] e^{-i(2+|f_0|^2)z}, \quad |\delta_m| \ll |f_0|, \quad (15)$$

we obtain real eigenvalues

$$\lambda^2 = \left( |f_0|^2 - 4 \sin^2 \frac{\chi_m}{2} \right)^2 - |f_0|^4 \geq 0 \quad (16)$$

only at the power of the wave beam equal to

$$\mathcal{P} \equiv 2N|f_0|^2 \leq \mathcal{P}_{\text{cr1}} = 4N \sin^2 \frac{\pi}{2N} \underset{N \gg 1}{\approx} \frac{\pi^2}{N}. \quad (17)$$

Thus the injected wave beam with the power  $\mathcal{P} > \mathcal{P}_{\text{cr1}}$  will be unstable with respect to azimuthal perturbations. Moreover, the critical power  $\mathcal{P}_{\text{cr1}}$  is not large and tends to zero as the number of cores on the ring of the multicore fiber increases ( $N \rightarrow \infty$ ).

The difference between the discrete and the continuous cases is related to the fact that in a continuous medium a plane wave is subject to filamentation instability at an arbitrarily small amplitude. This is not difficult to see from formula (17) for  $N \rightarrow \infty$ . The appearance of a threshold for a finite  $N$  is associated with the absence of perturbations in the system with a wavelength greater than the size of the discrete system.

##### B. MCF with a central core ( $\chi \neq 0$ )

Let us consider the case when the central core is present ( $\chi \neq 0$ ) and the energy transfer between the central core and the ring becomes possible. In Sec. III it was shown that for a certain ratio of the initial amplitudes, Eq. (11), there will be no beating between the central core and the ring in the linear case ( $\mathcal{P} \ll 1$ ). Next, we analyze the influence of the media nonlinearity on the evolution of the wave beam in the MCF under consideration (see Fig. 1). We find stationary nonlinear distributions and obtain a solution in quadratures.

The presence of the integral of problem (13) allows us to reduce the dimension of the problem and analyze it in detail on the phase plane. Indeed, we can seek the solution of Eqs. (12) in the form

$$a = \sqrt{\mathcal{P}A} e^{i(\phi+\theta)}, \quad u_n = \sqrt{\frac{\mathcal{P}(1-A)}{2N}} e^{i\phi}. \quad (18)$$

Here  $A$  is the fraction of the power in the central core. The change of wave beam parameters  $\{A, \theta, \phi\}$  along the propagation path satisfies the following system of ordinary differential equations:

$$\frac{dA}{dz} = -2\chi \sqrt{2N} \sqrt{A - A^2} \sin \theta, \quad (19a)$$

$$\frac{d\theta}{dz} = \sqrt{2N} \chi \frac{2A - 1}{\sqrt{A - A^2}} \cos \theta - \frac{(2N + 1)\mathcal{P}A}{2N} + \frac{\mathcal{P}}{2N} + 2, \quad (19b)$$

$$\frac{d\phi}{dz} = -2\chi \sqrt{2N} \sqrt{A - A^2} - \frac{\mathcal{P}^2}{4N} [(A - 1)^2 + 2NA^2] + 2(A - 1). \quad (19c)$$

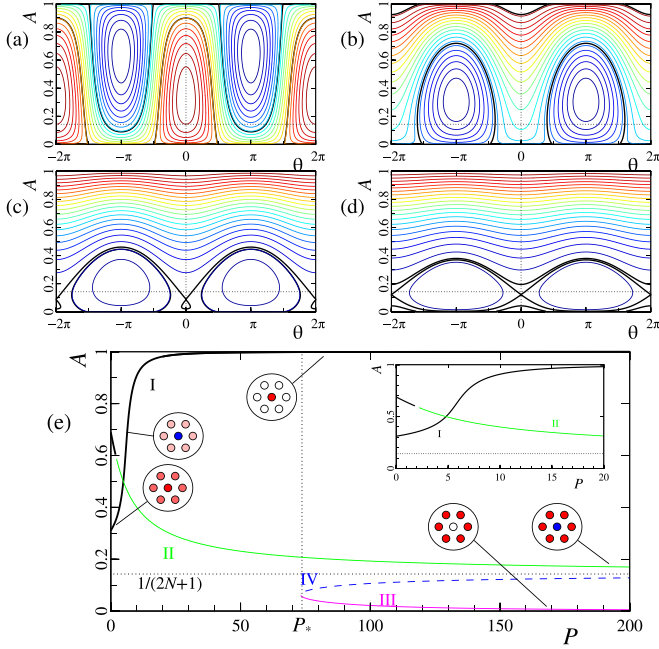


FIG. 2. (a)–(d) Phase plane of Eqs. (19a) and (19b) for the case of  $N = 3$  and  $\chi = 1$  for different power values,  $\mathcal{P} = 1$  (a), 20 (b), 40 (c), and 150 (d). The thick lines show separatrices. The dot line at  $A = 1/(2N + 1)$  denotes the homogeneous distribution for  $\theta = 0$ . (e) The equilibrium states of the system as a function of the power  $\mathcal{P}$ . The blue dashed line shows an unstable equilibrium state of the saddle type. The vertical line shows the position of the bifurcation point  $\mathcal{P}_* \approx 6\sqrt{3}N^2$ . The solid black lines show azimuthally stable solutions. The insets show examples of the transverse structure of the solution.

Equation (19c) for evolution of the phase  $\phi$  is separated from the dynamics of other parameters ( $A, \theta$ ). The two remaining equations (19a), (19b) have the integral of motion, i.e., the Hamiltonian

$$\mathcal{H} = 2\mathcal{P}\chi\sqrt{2NA(1-A)}\cos\theta - 2\mathcal{P}A + \frac{\mathcal{P}^2}{4N}[(A-1)^2 + 2NA^2] = \text{const.} \quad (20)$$

This allows us to write their solution in quadratures.

Let us analyze possible types of solutions of Eqs. (19a) and (19b) on the phase plane, the form of which depends essentially on the power of the wave beam  $\mathcal{P}$  injected into the MCF. As follows from Eq. (19a), there are two distributed equilibrium states of the saddle type ( $A = 0$  and  $A = 1$ ), the positions of which do not depend on the input power. These are degenerate one-dimensional manifolds that correspond to the localization of the field only in the central core (for  $A = 1$ ), or only on the ring of a multicore fiber (for  $A = 0$ , see Sec. IV A).

The phase plane in the case of a small input power  $\mathcal{P}$  of the injected wave beam is shown in Fig. 2(a). The thick curves denote the separatrices. It is seen that Eqs. (19a) and (19b) have four equilibrium states: two distributed equilibrium states of the saddle type ( $A = 0$  and  $A = 1$ ) and two centers. At low powers ( $\mathcal{P} \rightarrow 0$ ), these centers  $A_I, A_{II}$  approach the

values

$$A_I^0 = \frac{1}{2} - \frac{1}{2\sqrt{2N\chi^2 + 1}}, \quad \theta = 0, \quad (21a)$$

$$A_{II}^0 = \frac{1}{2} + \frac{1}{2\sqrt{2N\chi^2 + 1}}, \quad \theta = \pi, \quad (21b)$$

corresponding to the eigenvectors of the normal modes of the linear problem, Eq. (11).

As the wave beam power increases [see Fig. 2(b)], the positions of the centers will shift. The center at  $\theta = 0$  shifts up and the center at  $\theta = \pi$  shifts down. In this case, the motion outside the equilibrium states describes the successive transfer of energy from the central core (decrease of  $A$ ) to the ring of the multicore fiber and vice versa. Moreover, beats occur with a significant amplitude if the initial fraction of the energy in the central core  $A$  is not close to the stationary value  $A_I$  or  $A_{II}$ .

With an increase in the power up to the level

$$\mathcal{P}_* \approx 6\chi\sqrt{3}N^2 - 6N - \frac{2 + \chi^2 + 2\sqrt{3}\chi}{2\sqrt{3}\chi}, \quad (22)$$

a bifurcation occurs, and a new pair of equilibrium states appears: the center and the saddle type [see Fig. 2(c)]. With a further increase in power, the position of the born equilibrium state of the center type will shift to small values [ $A \rightarrow 0$ ; see Fig. 2(d)]. It can be seen from the insets in Figs. 2(c) and 2(d) that for a power of  $\mathcal{P} > \mathcal{P}_*$  the fraction of beating energy drops, and solutions with a small varying amplitude appear (centers near the maximum and minimum amplitudes). This solution corresponds to the capture of the field only in the central core or only in the ring because of the discreteness of the problem.

Figure 2(e) shows the dependence of all equilibrium states on the power  $\mathcal{P}$ . The insets of this figure show examples of the transverse structure of the solutions (the blue color denotes the field with the opposite sign). For the power  $\mathcal{P} \gg 1$ , one can find the asymptotics of the three equilibrium states of the center type

$$A_I \approx 1 - \frac{2\chi^2 N}{C^2}, \quad \theta = 0, \quad (23a)$$

$$A_{II} \approx \frac{1}{2N+1} + \frac{4\chi N^2 + (4-2\chi)N}{(2N+1)C}, \quad \theta = \pi, \quad (23b)$$

$$A_{III} \approx \frac{8\chi^2 N^3}{C^2}, \quad \theta = 0. \quad (23c)$$

Note that the branch  $A_{II}$  tends to the homogeneous intensity distribution  $|a|^2 = |f_0|^2$  having  $A = 1/(2N + 1)$ . Asymptotic (23c) is obtained for

$$\mathcal{P} \gg \mathcal{P}_* > 6\chi N^2 \gg 4. \quad (24)$$

Such a detailed analysis of Eqs. (19a) and (19b) also makes it possible to clarify the issue left unexplained in [19,20]. At first sight, this system has two more equilibrium states of the center type than the number of saddle points. Such a situation is impossible in a conservative system, since its Poincaré index (the difference in the number of centers and saddles) cannot exceed 1. To resolve this paradox, one should take into account two degenerate saddle-type manifolds (the lines at  $A = 0$  and  $A = 1$ ) leading the Poincaré index to zero.

### C. Stability analysis

Let us further analyze the stability of the solutions found with respect to the azimuthal perturbations on the ring of a multicore fiber. To do this, we assume that the wave field is a superposition of the solution found at a stationary point and a small perturbation on the ring

$$u_n = (f_0 + \delta u_m) e^{i\lambda z}, \quad |f_0|^2 = \frac{\mathcal{P}(1-A)}{2N}, \quad \lambda = \frac{d\phi}{dz}, \quad (25)$$

where the phase  $\phi$  is determined by Eq. (19c). Substituting the expression (25) into the system of equations (3) and linearizing with respect to small perturbations, we obtain a system of equations for  $\delta u_m$  in the first order of smallness

$$i \frac{d\delta u_m}{dz} = \lambda \delta u_m + (\delta u_m)_{n+1} + (\delta u_m)_{n-1} + f_0^2 \delta u_m^* + 2|f_0|^2 \delta u_m, \quad (26a)$$

$$-i \frac{d\delta u_m^*}{dz} = \lambda \delta u_m^* + (\delta u_m^*)_{n+1} + (\delta u_m^*)_{n-1} + f_0^{*2} \delta u_m + 2|f_0|^2 \delta u_m^*. \quad (26b)$$

We seek a solution of Eqs. (26) in the form  $\delta u_m, \delta u_m^* \propto e^{hz+i\kappa_m n}$ . As a result, we obtain an algebraic system of two homogeneous equations

$$\delta u_m (ih - \lambda - 2 \cos \kappa_m - 2|f_0|^2) - f_0^2 \delta u_m^* = 0, \quad (27a)$$

$$f_0^{*2} \delta u_m + \delta u_m^* (ih + \lambda + 2 \cos \kappa_m + 2|f_0|^2) = 0, \quad (27b)$$

which has a nontrivial solution in the case when  $h$  and  $\kappa_m$  satisfy the following dispersion relation:

$$h^2 = -(\lambda + 2 \cos \kappa_m + |f_0|^2)(\lambda + 2 \cos \kappa_m + 3|f_0|^2). \quad (28)$$

As shown in Sec. IV B, there exist three stationary solutions (23) for the isotropic distributions of the wave field, which correspond to the stationary points of the center type. We will analyze the stability of these solutions using the obtained dispersion relation (28). Here, we need to use expression (19c) with the values  $A$  and  $\theta$ , which characterizes corresponding distribution (23), to determine the parameter  $\lambda = d\phi/dz$ .

Let us first consider branch (23a), which describes the propagation of the wave field mainly in the central core [see Fig. 2(e)]. In this case, the expression for the parameter  $\lambda$  has the form

$$\lambda = 2(A-1) - \frac{\mathcal{P}}{2N} [(A-1)^2 + 2NA^2] - 2\chi \sqrt{2NA(1-A)}. \quad (29)$$

Substituting the approximation for the stationary point, Eq. (23a), into expressions (28) and (29) we find that branch I, localized at the center, is always stable:

$$h^2 \approx - \left( \mathcal{P} + 2 \cos \kappa_m + \frac{\chi^2}{\mathcal{P}} \right) \times \left( -\mathcal{P} + 2 \cos \kappa_m + \frac{3\chi^2}{\mathcal{P}} \right) < 0. \quad (30)$$

For branch III, localized in the ring [see Fig. 2(e)] from the approximation (23c), we find the parameter  $\lambda \simeq -2 - \mathcal{P}/2N$ . As a result, we get that branch III is always *unstable* in the field of existence

$$h^2 \approx \left( 4 \sin^2 \frac{\kappa_m}{2} + \frac{4N^2 \chi^2}{\mathcal{P}} \right) \times \left( \frac{\mathcal{P}}{N} - 4 \sin^2 \frac{\kappa_m}{4} - \frac{12N^2 \chi^2}{\mathcal{P}} \right) > 0. \quad (31)$$

Finally, consider branch II [Eq. (23b)] for which the parameter  $\lambda$  is equal to

$$\lambda = 2(A-1) - \frac{\mathcal{P}}{2N} [(A-1)^2 + 2NA^2] + 2\chi \sqrt{2NA(1-A)}. \quad (32)$$

It is difficult to make an accurate analytical analysis of the stability of this wave-field distribution. However, substituting the limiting value  $A \approx 1/(2N+1)$ , we find

$$\lambda \approx -\frac{\mathcal{P}}{2N+1}, \quad |f_0|^2 \approx \frac{\mathcal{P}}{2N+1}, \quad (33a)$$

$$h^2 \approx -4 \left( \frac{\mathcal{P}}{2N+1} + \cos \frac{\pi m}{N} \right) \cos \frac{\pi m}{N}. \quad (33b)$$

The value of  $h^2$  becomes positive when

$$\mathcal{P} \gtrsim (2N+1) \sin \frac{\pi}{2N} \underset{N \gg 1}{\approx} \pi. \quad (34)$$

This is a rough estimate. Nevertheless, it differs from the numerically found threshold by no more than 1.5 times.

The bold black lines in Fig. 2(e) show the wave field distributions which are stable with respect to the azimuthal perturbations. Numerical simulation of the initial system of equations (3) confirms the above analysis.

In conclusion, it should be noted that the found isotropic distribution of Eq. (23) [see Fig. 2(e)] is not suitable for transporting a wave beam with a power greater than the critical one for the self-focusing [19,20]. Branches II and III are destroyed at high powers due to azimuthal perturbations. The wave field in branch I at high powers is concentrated only in the central core; thus its power is limited to a value of the order of the critical self-focusing power, Eq. (5).

### V. MIRROR-SYMMETRIC DISTRIBUTIONS

Next, let us consider nonisotropic configurations of the wave field distributions in the MCF in order to use a larger number of cores for transporting higher powers. In addition to the solution in the form of the isotropic distribution and a central core (see Sec. IV B), Eqs. (3) have a closed solution in the form of a superposition of all odd linear modes (with odd numbers  $m = 1, 3, 5, \dots$ ) over the ring of the multicore fiber. It should be noted that odd modes cannot excite even modes or a field in the central core. This allows us to use MFCs with cores located only on the ring. Analysis of the corresponding equations for an arbitrary number  $N$  (there are  $2N$  cores on the ring) is difficult. However, the case of  $N = 3$  can be analyzed rather easily, since in this case there are only three odd linear modes, specifically,  $f_1 e^{i\frac{n\pi}{3}}$ ,  $f_5 e^{-i\frac{n\pi}{3}}$ ,

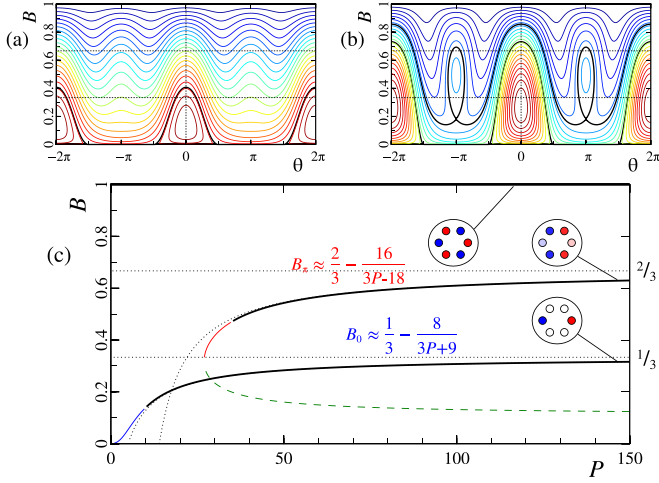


FIG. 3. (a),(b) Phase plane of system of equations (38) for different power values  $\mathcal{P} = 10$  (a) and  $40$  (b). The bold lines show the separatrices. The dot line corresponds to the distribution of the field with the maximal localization. (c) Equilibrium states of the system as functions of the power  $\mathcal{P}$ . The solid bold curves show the azimuthally stable solutions. The insets show examples of the transverse structure of the solution.

and  $f_N e^{in\pi}$ . Since we are looking for stationary distributions, the amplitudes of the  $f_1$  and  $f_5$  modes must coincide ( $|f_1| = |f_5|$ ). Then, the system of equations (3) can be described by two complex amplitudes of the first and the third modes:

$$u_n = f_1(z) \cos \frac{n\pi}{3} + (-1)^n f_N(z). \quad (35)$$

The power conservation law in this case has the form

$$\mathcal{P} = 3|f_1|^2 + 6|f_N|^2 = \text{const}. \quad (36)$$

The presence of conservation law (36) allows us to reduce the dimension of the problem. So, we seek the solution of equations (3) in the form

$$f_1 = \sqrt{\frac{\mathcal{P}}{3}}(1-B)e^{i\phi}, \quad f_N = \sqrt{\frac{\mathcal{P}B}{6}}e^{i(\phi+\theta)}, \quad (37)$$

where  $B$  is the power fraction in the  $(-1)^n$  mode and  $\theta$  is the relative phase difference between the first and third modes. Substituting the fields in the form of Eq. (37) into Eqs. (3), we obtain the following system of ordinary differential equations for parameters  $\{B, \theta\}$ :

$$\frac{dB}{dz} = -\frac{\mathcal{P}(1-B)}{3} \left[ \sqrt{\frac{B-B^2}{2}} \sin \theta - B \sin 2\theta \right], \quad (38a)$$

$$\begin{aligned} \frac{d\theta}{dz} = & \frac{\mathcal{P}}{6}(4B-1) \sqrt{\frac{1-B}{2B}} \cos \theta + \frac{\mathcal{P}}{6}(2B-1) \cos 2\theta \\ & + \frac{\mathcal{P}B}{4} - \frac{\mathcal{P}}{12} + 3. \end{aligned} \quad (38b)$$

Let us analyze the phase plane of equations (38), which essentially depends on the power of the wave beam  $\mathcal{P}$  [Figs. 3(a) and 3(b)]. As before, there are two degenerate manifolds ( $B = 0$ ,  $B = 1$ ) whose positions do not depend on the power of the wave field. The case of  $B = 0$  corresponds to an azimuthally

unstable distribution over a ring according to the law  $u_n = \sqrt{\mathcal{P}} \cos \frac{n\pi}{3} e^{i\phi}$ . The case of  $B = 1$  corresponds to the stable field distribution  $u_n = (-1)^n \sqrt{\mathcal{P}/2} e^{i\phi}$ . The equilibrium states are shown in Fig. 3(c) as a function of the power  $\mathcal{P}$ .

Already at the power  $\mathcal{P} = 0$ , the center-saddle-creation bifurcation near  $B \simeq 0$  occurs at  $\theta = 0$  [see Fig. 3(a)]. This corresponds to the appearance of the lower branch  $B_0$  in Fig. 3(c). As the power of the wave beam  $\mathcal{P}$  increases, the position of this equilibrium state is rapidly shifted upwards according to the law

$$B_0 \approx \frac{\mathcal{P}^2}{648} \quad \text{at } \mathcal{P} \ll 10. \quad (39)$$

In this case, the wave field dynamics is similar to the isotropic case (Fig. 2). The value of  $B$  decreases and increases periodically (its ‘‘beating’’ occurs). Consequently, the coherent wave field could not be localized in several selected cores at low levels of the power  $\mathcal{P}$ . The second bifurcation occurs at the wave field power  $\mathcal{P} \simeq 27$  [see Fig. 3(b)], where new equilibrium states (center and saddle) appear at  $\theta = \pi$ . At a given power, the upper branch  $B_\pi$  appears in Fig. 3(c).

As the wave beam power increases, the equilibrium state at  $\theta = 0$  tends to  $B \simeq 1/3$  according to the law

$$B_0 \approx \frac{1}{3} - \frac{8}{3\mathcal{P}+9}. \quad (40)$$

This corresponds to the fact that the field is localized mainly in two opposite cores [see the inset in Fig. 3(c)]. The second equilibrium state at  $\theta = \pi$  tends to  $B \simeq 2/3$  with an increasing power according to the law

$$B_\pi \approx \frac{2}{3} - \frac{16}{3\mathcal{P}-18}. \quad (41)$$

This branch corresponds to the wave beam distributed in the four cores of the MCF under consideration.

Thus, in the case of six core fibers ( $N = 3$ ,  $\chi = 0$ ), there are two branches of the solutions [see Fig. 3(c)], which consist of the odd modes only [ $\cos \frac{n\pi}{3}$  and  $(-1)^n$ ] and describe the stationary wave field distributions on the ring of the multicore fiber. It should be noted that the second branch  $B_\pi$  has a threshold character, since it exists only at relatively high powers ( $\mathcal{P} \gtrsim 27$ ). The wave field on the branches  $B_0$  and  $B_\pi$  at large powers is concentrated mainly in two and four cores, respectively. Hence the  $B_\pi$  branch is preferable for coherent propagation of a high-power wave beam in a multicore fiber.

An analytic study of the stability of the solutions  $B_0$  and  $B_\pi$  is a rather complicated problem. However, in this case it is easy to find the azimuthal stability threshold by direct numerical simulation. As shown by numerical analysis with initial noise level of  $10^{-5}$ , the  $B_0$  and  $B_\pi$  modes are stable at the powers of  $\mathcal{P} \gtrsim 10$  and  $\mathcal{P} \gtrsim 40$ , respectively. The solid thick lines in Fig. 3(c) show modes that are stable to azimuthal perturbations.

## VI. CROWNLIKE DISTRIBUTIONS

Let us study another possible configuration of a wave beam in a multicore optical fiber consisting of a large number of cores (the restriction on the number of cores is limited only by technological and geometric possibilities) on the ring with

allowance for the central core, with the aim of aggregating an even larger number of cores for coherent propagation of a high-power laser beam.

To do this, we consider the limiting case, where the distribution of the wave field on the ring has a modulation through the core:

$$u_n = f_0 + (-1)^n f_N. \quad (42)$$

This corresponds to the case of superposition of linear modes with  $m = 0$  and  $m = N$ . The power conservation law for such distribution has the form

$$\mathcal{P} = |a|^2 + 2N(|f_0|^2 + |f_N|^2). \quad (43)$$

The presence of this integral allows us once more to reduce the dimensionality of the problem and to seek the beam distribution in a multicore fiber in the form

$$a = \sqrt{\mathcal{P}A} e^{i(\xi+\theta)}, \quad (44a)$$

$$u_n = \sqrt{\frac{\mathcal{P}(1-A-B)}{2N}} e^{i\xi} + (-1)^n \sqrt{\frac{\mathcal{P}B}{2N}} e^{i(\xi+\phi)}, \quad (44b)$$

where  $A$  and  $B$  are the fractions of the power in the central core and in the mode  $(-1)^n$ , respectively, and  $\phi$  and  $\theta$  are the relative phase differences. Substituting the fields in the form of Eq. (44) into Eqs. (3), we obtain the following system of ordinary differential equations for the wave field parameters:

$$\frac{dB}{dz} = -\frac{\mathcal{P}}{N} B(1-A-B) \sin 2\phi, \quad (45a)$$

$$\frac{d\phi}{dz} = 4 + \frac{\mathcal{P}}{N} (2B+A-1) \cos^2 \phi + \sqrt{\frac{2N\chi^2 A}{1-A-B}} \cos \theta, \quad (45b)$$

$$\frac{dA}{dz} = -2\chi \sqrt{2NA(1-A-B)} \sin \theta, \quad (45c)$$

$$\begin{aligned} \frac{d\theta}{dz} = 2 + \frac{\chi \sqrt{2N} \cos \theta}{A(1-A-B)} (B+2A-1) \\ + \frac{\mathcal{P}}{2N} [2B \cos^2 \phi + 1 - A(2N+1)]. \end{aligned} \quad (45d)$$

Analysis of the resulting *four-dimensional* system (45) is difficult. However, we can find the stationary points and investigate them for stability.

The case of the stationary state  $B = 0$  for any value of the phase  $\phi$  corresponds to the injection of a wave beam into the central core and a uniform distribution of the wave field on the ring of a multicore fiber. This situation was studied earlier in Sec. IV B.

The case of the stationary state  $A + B = 1$  corresponds to the situation of the injection of a wave field into the central core and the excitation of the linear mode  $(-1)^n$  on the ring of a multicore fiber. It should be noted that these two modes do not interact. Consequently, the wave fields on the ring and at the center are not coherent. In this regime, a wave field of arbitrary power can propagate, since such a configuration of the wave field is stable with respect to the azimuthal perturbations, but the fractions of the energies in the two subsystems could not be synchronized.

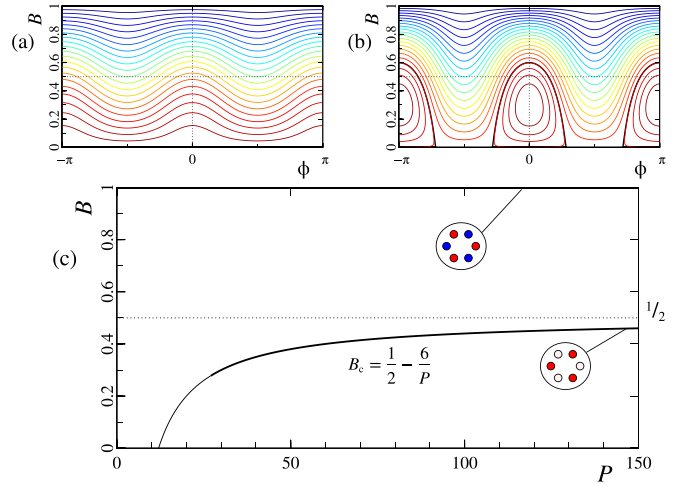


FIG. 4. (a),(b) Phase plane of Eqs. (45a) and (45b) for  $A = 0$  and  $N = 3$  and different powers  $\mathcal{P} = 10$  (a) and  $30$  (b). The bold lines show the separatrices. (c) The equilibrium states of the system as functions of the power  $\mathcal{P}$ . Solid bold black lines show azimuthally stable solutions. The insets show examples of the transverse structure of the solution.

We now consider the case of the stationary state  $A = 0$  corresponding to the absence of a central core in the MCF. Analysis of Eqs. (45a) and (45b) shows the existence of an equilibrium state

$$B_c = \frac{1}{2} - \frac{2N}{\mathcal{P}}, \quad \phi = 0, \quad A = 0. \quad (46)$$

This solution has a threshold character, i.e., it exists for  $\mathcal{P} > \mathcal{P}_* = 4N$ . Figure 4 shows the corresponding phase plane. Only the beats between the linear modes  $f_0$ ,  $(-1)^n f_N$  are present at low wave beam powers  $\mathcal{P} < \mathcal{P}_*$ . This disallows one to concentrate the radiation in several selected cores. The bifurcation of center-saddle creation and a change in the stability of the manifold  $A = B = 0$  occur at the power  $\mathcal{P} = \mathcal{P}_*$ . With a further increase in the wave beam power  $\mathcal{P}$ , the position of the center shifts upward to the value  $B = 1/2$  [see Eq. (46)]. The black solid line in Fig. 4(c) shows the dependence of the equilibrium state on the power  $\mathcal{P}$  for  $N = 3$ . A numerical analysis of the  $B_c$  mode shows its azimuthal stability for  $\mathcal{P} \geq 10N > \mathcal{P}_*$  in the MCF without a central core ( $\chi = 0$ ). Adding of the central core introduces a new scattering channel, which leads to a noticeable increase in the azimuthal stability threshold of the mode  $\mathcal{P} \geq 10(1 + \chi)N$ .

Let us consider now a more general case, where both  $A$  and  $B$  are not equal to zero. The stationary points are located at (1)  $\phi = 0$ ,  $\theta = 0$ , and (2)  $\phi = 0$ ,  $\theta = \pi$ . However, a point with  $\theta = 0$  corresponds to an unstable equilibrium state of saddle type and is therefore not of interest to us. The asymptotic behavior of the second state at large powers  $\mathcal{P}$  has the form

$$A_- \approx \frac{1}{N+1} + \frac{\chi N(N-2)}{\mathcal{P}(N+1)}, \quad (47a)$$

$$B_- \approx \frac{N}{2(N+1)} - \frac{N[(4-\chi)N+4-3\chi]}{2\mathcal{P}(N+1)}. \quad (47b)$$

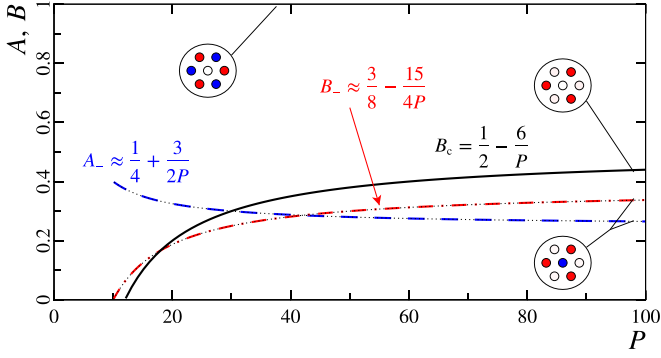


FIG. 5. Dependence of the equilibrium states  $A$  and  $B$  on the power  $\mathcal{P}$  (43). Here, the red dot-dashed and blue dashed curves show the dependence of the power fraction in the central core and in the  $(-1)^n$  mode, respectively. The insets show the sample wave field distribution. A black solid curve shows the dependence (46) for the case where there is no radiation injected into the central core.

Thus the central core can be used to transport a high-power wave beam in a multicore fiber. Note that this solution exists only for the powers

$$\mathcal{P} > (4 - \chi)N + 4 - 3\chi, \quad (48)$$

i.e., it has a threshold character, as in the case of the mode described by Eq. (46). The numerically found values of the  $A_-$  and  $B_-$  modes agree well with the asymptotic, Eq. (47), in the entire power range (see Fig. 5). Here, the red dash-dotted line shows dependence (43) of the power fraction in the central core on the total power  $\mathcal{P}$ , and the blue dot-dashed line shows the dependence of the power fraction in the linear mode  $(-1)^n$  of the total power  $\mathcal{P}$ . Numerical analysis shows that the solution found for Eq. (47) is stable with respect to the azimuthal perturbations only at sufficiently high powers  $\mathcal{P} > 20(N + 1)$  for  $\chi = 1$  and initial noise level of  $10^{-5}$ .

To conclude this section, Fig. 6 shows the amplitudes and wave field distributions in a multicore optical fiber for various powers of  $\mathcal{P}$  and the number of cores on the ring.

## VII. SUPREME MODE

Next, we analyze another configuration of the inhomogeneous wave field distribution in MCF in the absence of a central core ( $\chi = 0$ ):

$$u_n = (-1)^n f_N. \quad (49)$$

On the phase plane (Fig. 4), this wave field distribution corresponds to the manifold with  $B = 1$  and  $A = 0$ . Spatial distribution (49) is valuable from a practical point of view, since all available  $2N$  MCF cores are used to transport laser radiation.

Let us investigate the stability of wave field distribution (49) with respect to the azimuthal perturbations. To do this, we assume that the wave field is a superposition of solution (49) and a small perturbation having the form (recall that  $\kappa_m = \pi m/N$ )

$$u_n = [(-1)^n f_N + \delta_m e^{i\kappa_m n}] e^{i(2 - |f_N|^2)z}, \quad |\delta_m| \ll |f_N|.$$

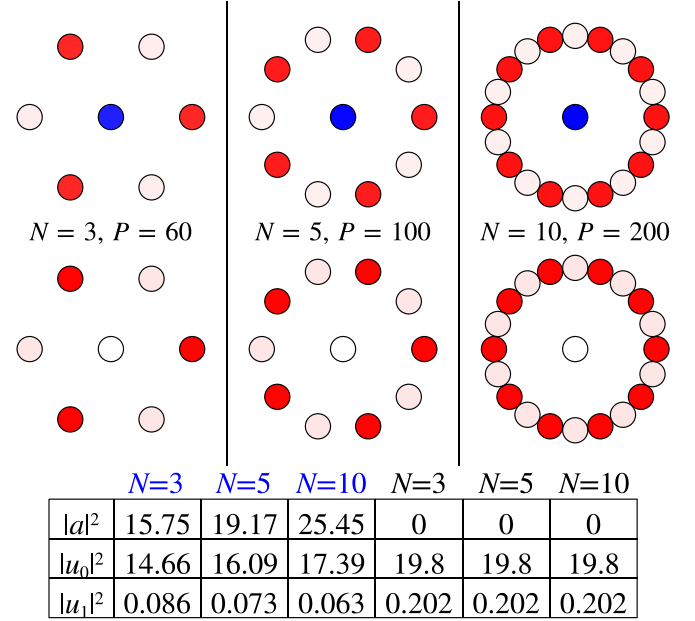


FIG. 6. Wave field distribution for different powers  $\mathcal{P}$  and the number of the cores on a ring. The coupling coefficient is  $\chi = 1$ . The blue color denotes the field with the opposite sign. The table shows the field intensities in each core.

Substituting this expression in the system of equations (3) and linearizing with respect to small perturbations, we obtain a system of equations for  $\delta_m$  in the first order of smallness:

$$i \frac{d\delta_m}{dz} = 2\delta_m + 2\delta_m \cos \kappa_m + f_N^2 \delta_m^* + |f_N|^2 \delta_m, \quad (50a)$$

$$-i \frac{d\delta_m^*}{dz} = 2\delta_m^* + 2\delta_m^* \cos \kappa_m + f_N^{*2} \delta_m + |f_N|^2 \delta_m^*. \quad (50b)$$

We seek a solution of Eqs. (50) in the form  $\delta_m, \delta_m^* \propto e^{i\lambda z}$ . As a result, we obtain an algebraic system of two homogeneous equations,

$$\delta_m \left( \lambda + 4 \cos^2 \frac{\kappa_m}{2} + |f_N|^2 \right) + f_N^2 \delta_m^* = 0, \quad (51a)$$

$$f_N^{*2} \delta_m + \delta_m^* \left( -\lambda + 4 \cos^2 \frac{\kappa_m}{2} + |f_N|^2 \right) = 0, \quad (51b)$$

which has a nontrivial solution in the case when  $\lambda$  and  $\kappa_m$  satisfy the following dispersion relation:

$$\lambda^2 = \left( 4 \cos^2 \frac{\kappa_m}{2} + |f_N|^2 \right)^2 - |f_N|^4 \geq 0.$$

This means that perturbations will not increase and the nonlinear solution  $u_n = (-1)^n f_N$  is stable for any amplitudes  $f_N$ .

Numerical analysis of nonlinear dynamics in a multicore fiber of six cores ( $N = 3$ ) confirms the stability of the nonlinear solution found. The results of numerical simulation clearly demonstrate that even noises with an amplitude of tens of percents of the amplitude of the nonlinear solution  $f_N$  do not have a noticeable effect on the dynamics of the wave field in the MCF. Only small beatings having the amplitude of the wave field occur. Moreover, the solution found is also stable with respect to random perturbations (up to 10%)

of the refractive index in each of the cores. Moreover, the threshold for the amplitude of permissible perturbations of the MCF structure increases with the increasing amplitude of the nonlinear solution  $f_N$ .

Thus supreme nonlinear mode (49), which is stable with respect to azimuth disturbances, is an attractive object for coherent propagation of laser radiation in MCF, with a total power significantly higher than that capable of being transmitted in a single-core fiber.

### VIII. COMPARISON WITH DIRECT SIMULATIONS

To verify the stability of the analytic solutions found above in the frame of the single-mode approximation, we performed numerical simulation of the wave field dynamics described by the nonlinear unidirectional wave propagation equation [24,25]

$$i \frac{\partial \mathcal{E}}{\partial z} = \sqrt{k_0^2 n_0^2 + \Delta_\perp} \mathcal{E} + k_0 n_2 |\mathcal{E}|^2 \mathcal{E} + k_0 \delta n U(x, y) \mathcal{E}, \quad (52)$$

with the potential

$$U = \sum_n \exp \left( - \left[ \frac{(x - x_n)^2 + (y - y_n)^2}{r_n^2} \right]^2 \right).$$

Here  $x_n, y_n, r_n$  are the position and radius of the cores,  $n_0$  is the refractive index of the cladding,  $\delta n$  is the difference between the refractive indices of the cores and the medium, and  $n_2$  is the nonlinear refractive index. The operator  $\sqrt{k_0^2 n_0^2 + \Delta_\perp}$  can be easily calculated in Fourier space and allows one to properly describe wave fields with transverse scales of order of the wavelength by taking into account spherical aberrations.

The calculations were carried out with the help of the code [26] at a wavelength  $2\pi/k_0 = 1.03 \mu\text{m}$  for a silica fiber, similar to ones available to our group. The refractive index of the cladding was taken to be  $n_0 = 1.45$ . The difference in the refractive indices between the cores and the cladding was  $\delta n = 0.002$ . The nonlinear refractive index was  $n_2 = 3 \times 10^{-16} \text{ cm}^2/\text{W}$ . The radii of the cores were equal to  $r_n = 4 \mu\text{m}$  and the distance between them was  $15 \mu\text{m}$ . The fields in each core were set in the form of a Gaussian function closest to the mode field  $\text{LP}_{01}$  of an individual core. The simulation was performed on a grid with the number of points  $256 \times 256$  in a plane perpendicular to the propagation direction with step  $\Delta x = \Delta y = 0.4 \mu\text{m}$ . The calculation step along the fiber axis was chosen to be  $\Delta z = 5 \mu\text{m}$ . We have verified that reducing the step by half (with a corresponding increase in the number of points along any coordinate) does not lead to a change in the calculation results.

The initial wave field distributions were chosen as the limiting distributions (for  $\mathcal{P} \rightarrow \infty$ ) of the found analytic solution. This significantly simplified the form of the initial distribution, but introduced appreciable noise up to the level of 5% of the amplitude of the exact solution. Since the presented solutions are stable, then such simplification did not lead to a noticeable distortion of the wave field structure, but gave only small amplitude and phase oscillations. The amplitude of the wave field was chosen so that the power in each core was of 0.7 critical power of self-focusing in fused silica. Higher

powers lead to the appearance of thermal effects that can damage the considered fiber.

Direct numerical simulation of Eq. (52) showed the good stability of most of the found solutions: the mode  $B_0$  [Fig. 7(a)], the mode  $B_c$  [Fig. 7(c)], and the supreme mode  $(-1)^n$  [Fig. 7(d)]. Note that the total power in all the presented calculations exceeded the critical self-focusing power in the medium. Moreover, the calculations showed the possibility of coherent transport of a wave beam with a power of seven critical powers of self-focusing using the supreme mode of 10-core fiber.

The use of powers close to the critical power of self-focusing leads to the nonlinear narrowing of the wave field inside cores. This provides the nonlinear decrease of the coupling coefficient  $\chi$  and effective increase of the dimensionless power  $\mathcal{P} \propto |\mathcal{A}|^2/\chi$ . Therefore, the found nonlinear solutions become only more stable if one takes into account the narrowing. This is also demonstrated by direct numerical simulation of Eq. (52).

The case of the mode  $B_\pi$  is more complicated. The interaction of cores through one (unaccounted for in our simple analytical model) becomes noticeable at small distances between the cores [see Fig. 7(b)]. This leads to a periodic synchronous phase oscillation of half of the cores relative to another half. Such behavior of the phase dynamics is the consequence of the beats of the complex amplitude of two linearly coupled stable groups of cores.

### IX. CONCLUSION

A detailed analysis of the self-action of wave beams in a small-sized multicore fiber consisting of  $2N$  identical cores located along a ring at equal distances from each other and a separated core in the center is carried out. Exact analytical solutions for the wave field distributions in the nonlinear regime are obtained. This includes both the known solution, localized in a single core, and the solutions using all the light guides [the  $(-1)^n$  mode], half of them (crownlike distribution), or only a small fraction of the cores (mirror-symmetric distributions). Their stability is shown analytically and numerically, which makes it possible to use such wave field distributions for coherent radiation transport in several parallel optical fibers for arbitrarily large distances. In this case, the total power can exceed by many times the critical power of self-focusing in the medium.

The case of isotropic wave field distributions is analyzed in detail. A critical power is found, up to which the homogeneous distributions are stable. Actually, this critical power gives the upper limit, to which the most easily excited isotropic distributions can be used to transmit the coherent signal in the considered multicore fibers.

The stability of the most interesting nonlinear wave field distribution  $(-1)^n f_N$  with respect to field perturbations and deformation of the MCF structure is studied. Such a nonlinear solution is distributed over the largest number of MCF cores and, accordingly, has the maximum power for a given field amplitude. It is shown that this nonlinear distribution is asymptotically stable at a high radiation power and at even not too small (up to 10%) perturbations of the refractive index in various optical cores. This makes the spatial distribution

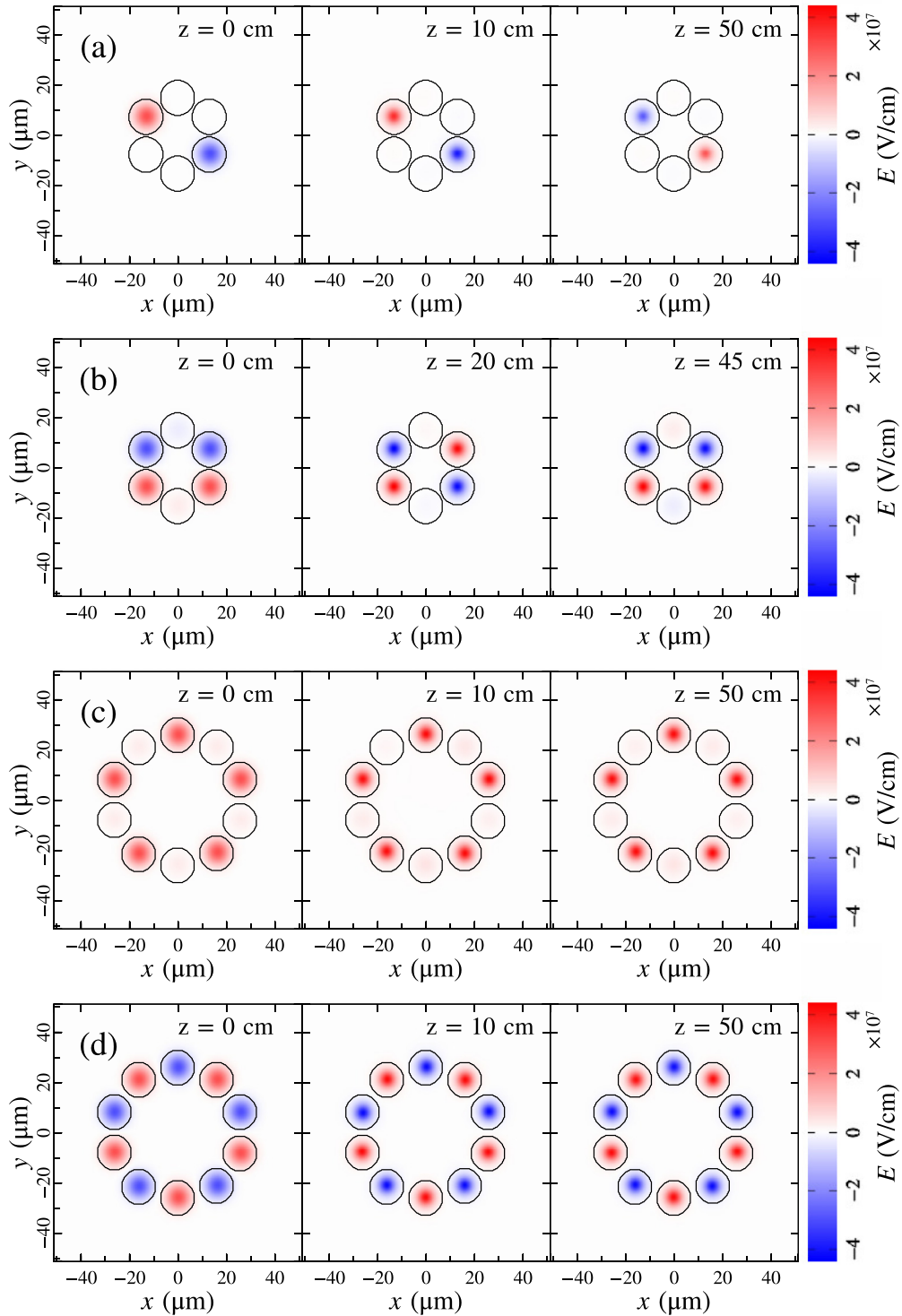


FIG. 7. Distributions of the real part of the wave fields corresponding to (a) the  $B_0$  mode (39) with total power  $1.4P_{cr}$ , (b) the  $B_\pi$  mode (41) with total power  $2.8P_{cr}$ , (c) the  $B_c$  mode (46) with total power  $3.5P_{cr}$ , and (d) the supreme mode (49) with total power  $7P_{cr}$ . Here  $P_{cr} \approx 5$  MW is the critical power of self-focusing in fused silica.

of supreme mode  $(-1)^n$  attractive for various applications, including the transport and self-compression of laser pulses in the MCF.

**ACKNOWLEDGMENT**

This work was supported by the Russian Science Foundation (Project No. 16-12-10472).

- [1] G. Mourou, T. Tajima, M. N. Quinbn, B. Brocklesby, and J. Limpert, *Nucl. Instrum. Methods Phys. Res., A* **740**, 17 (2014).
- [2] G. Mourou, B. Brocklesby, T. Tajima, and J. Limpert, *Nat. Photon.* **7**, 258 (2013).
- [3] M. Jiang, R. Su, Z. Zhang, Y. Ma, X. Wang, and P. Zhou, *Appl. Opt.* **56**, 4255 (2017).
- [4] Z. Huang, X. Tang, Y. Luo, C. Liu, J. Li, D. Zhang, X. Wang, T. Chen, and M. Han, *Rev. Sci. Instrum.* **87**, 033109 (2016).
- [5] D. N. Christodoulides, F. Lederer, and Y. Silberberg, *Nature (London)* **424**, 817 (2003).
- [6] Y. Kivshar and G. Agrawal, *Optical Solitons. From Fibers to Photonic Crystals* (Academic Press, New York, 2005).
- [7] A. Scott, *Nonlinear Science. Emergence and Dynamics of Coherent Structures* (Oxford University Press, Oxford, 2003).
- [8] T. X. Tran, D. C. Duong, and F. Biancalana, *Phys. Rev. A* **89**, 013826 (2014).
- [9] P. Panagiotopoulos, P. Whalen, M. Kolesik, and J. V. Moloney, *Nat. Photon.* **9**, 543 (2015).
- [10] A. M. Rubenchik, I. S. Chekhovskoy, M. P. Fedoruk *et al.*, *Opt. Lett.* **40**, 721 (2015).
- [11] A. A. Balakin, A. G. Litvak, V. A. Mironov, and S. A. Skobelev, *Laser Phys.* **28**, 045401 (2018).
- [12] T. X. Tran, D. C. Duong, and F. Biancalana, *Phys. Rev. A* **90**, 023857 (2014).
- [13] L. G. Wright, D. N. Christodoulides, and F. W. Wise, *Nat. Photon.* **9**, 306 (2015).
- [14] S. Minardi, F. Eilenberger, Y. V. Kartashov *et al.*, *Phys. Rev. Lett* **105**, 263901 (2010).
- [15] F. Eilenberger, St. Minardi, A. Szameit, U. Ropke, J. Kobelke, K. Schuster, H. Bartelt, S. Nolte, L. Torner, F. Lederer, A. Tunnermann, and T. Pertsch, *Phys. Rev. A* **84**, 013836 (2011).
- [16] D. Cheskis, S. Bar-Ad, R. Morandotti, J. S. Aitchison, H. S. Eisenberg, Y. Silberberg, and D. Ross, *Phys. Rev. Lett.* **91**, 223901 (2003).
- [17] D. N. Christodoulides and R. I. Joseph, *Opt. Lett.* **13**, 794 (1988).
- [18] A. A. Balakin, A. G. Litvak, V. A. Mironov, and S. A. Skobelev, *Phys. Rev. A* **94**, 063806 (2016).
- [19] S. K. Turitsyn, A. M. Rubenchik, M. P. Fedoruk, and E. Tkachenko, *Phys. Rev. A* **86**, 031804 (2012).
- [20] A. M. Rubenchik, E. V. Tkachenko, M. P. Fedoruk, and S. K. Turitsyn, *Opt. Lett.* **38**, 4232 (2013).
- [21] F. Lederer, G. I. Stegeman, D. N. Christodoulides, G. Assanto, M. Segev, and Y. Silberberg, *Phys. Rep.* **463**, 1 (2008).
- [22] F. Eilenberger, A. Szameit, and T. Pertsch, *Phys. Rev. A* **82**, 043802 (2010).
- [23] F. Y. M. Chan, A. Pak, T. Lau, and H.-Y. Tam, *Opt. Express* **20**, 4548 (2012).
- [24] S. N. Vlasov and V. I. Talanov, *Radiophys. Quantum Electron.* **38**, 1 (1995).
- [25] A. V. Husakou and J. Herrmann, *Phys. Rev. Lett.* **87**, 203901 (2001).
- [26] A. Andrianov, E. Anashkina, A. Kim, I. Meyerov, S. Lebedev, A. Sergeev, and G. Mourou, *Opt. Express* **22**, 28256 (2014).